IOP Publishing Journal of Physics D: Applied Physics
J. Phys. D: Appl. Phys. **52** (2019) 184002 (7pp) https://doi.org/10.1088/1361-6463/ab062f

Structural coarsening of magnetic ellipsoid particle suspensions driven in toggled fields

Hojin Kim, Jonathan L Bauer, Paula A Vasquez and Eric M Furst[1]

Department of Chemical and Biomolecular Engineering, University of Delaware, Newark, DE 19716, United States of America

E-mail: furst@udel.edu

Received 30 November 2018, revised 25 January 2019
Accepted for publication 11 February 2019
Published 1 March 2019

Abstract

The suspension structure of magnetic ellipsoid nanoparticles is studied as they are driven by toggled magnetic fields in a microgravity environment. Suspensions coarsen in the applied field, but do not phase separate fully due to attraction induced by their remenant magnetism. The structure and kinetics of coarsening depend on the aspect ratio of the particles. The coarsening of ellipsoids with aspect ratio $\alpha = 2$ depends on the field strength and toggle frequency. Longer ellipsoids ($\alpha = 4$) form long fibrous structures that aggregate laterally with kinetics that are less sensitive to the field conditions. These results suggest an interplay between colloidal interactions, particle shape, and driving field that can be used to control the suspension microstructure.

Keywords: assembly kinetics, magnetic colloids, self-assembly, anisotropic particle

Supplementary material for this article is available online

(Some figures may appear in colour only in the online journal)

1. Introduction

From the first observation of electrorheological (ER) fluids by Winslow [1], applications of ER fluids in hydraulic valves and pumps have been designed and to make use of their rapid transition from a fluid to a solid-like state in a strong electric field [2, 3]. Similarly, magnetorheological (MR) fluids, which operate on analogous principles in, but instead in magnetic fields, have been investigated and used in applications including dampers, clutches, and brakes [4, 5].

The field-induced formation of microstructure is crucial to the development of MR fluid-based materials and thus, understanding the microstructure formation kinetics in response to a magnetic field is required to improve their performance. Magnetic particles are subject to field-induced interaction and as a result of the interactions, they form chain-like structures [6, 7]. Chain–chain lateral attractions by thermal fluctuations lead to further aggregation and create denser, fibrous and percolated, networks [8]. Under steady (dc) fields, lateral aggregations among chains of particles stiffens as applying the field and decrease segmental motions of chains [9].

The fibrous, percolated gel-like state of an MR fluid is a kinetically arrested, nonequilibrium state which is not the most energetically favorable suspension microstructure. However, such jammed microstructures can be driven to evolve into an equilibrium state, a body-centered tetragonal (BCT) solid [10]. One means to reach this equilibrium from the gel-like state is to toggle the magnetic field [6, 7, 11, 12]. By repeatedly switching the field on and off, the suspension particles rearrange without fully redispersing. Promislow and Gast first showed that toggled magnetic fields lead to the evolution of an MR suspension microstructure. The suspension eventually forms elongated, droplet-like structures with conical spikes at the ends [11, 12]. In some cases, the phase separation kinetics follow a fluid-like coarsening, analogous to the Rayleigh–plateau breakup into the final 'droplet-like' phases [7, 13, 14].

Recently, the kinetics of the transition in toggled fields from a kinetically arrested phase into the equilibrium phase

[1] Author to whom any correspondence should be addressed.

have been clarified in microgravity experiments [6]. The growth of the microstructure first follows a diffusion-limited process, which is indicated by sub-unity exponent in a power law of the aggregate width evolution $\langle s(t)\rangle \sim t^z$, where z is the exponent of power law (typically $z \sim 0.3$, consistent with diffusion-mediated coarsening) and $\langle s(t)\rangle$ is the average aggregate size. After a period, which depends weakly on field strength and strongly on toggle frequency, the size of aggregated columns composed of paramagnetic colloids increases due to coalescence, resulting in growth with a super-unity exponent, $z \sim 1.5$.

Later, toggled magnetic fields were applied to observe details of the aggregated microstructure in ground experiments (under a normal gravitational force). These studies demonstrate that the pulse frequency plays a significant role in the crystallization of magnetic spheres [7]. In the case of high toggle frequencies, colloids cannot escape the kinetically arrested phase due to the short timescale of particle diffusion. Since colloids are too mobile under very low pulse frequencies to stay in the boundary where field-induced interaction is dominant over the Brownian diffusion, this condition is also not appropriate for particles to rearrange into the crystalline structure. In subsequent computational studies, Sherman and Swan showed that toggled interactions of particles lead to higher crystal quality with faster kinetics and the crystal growing mechanism is tunable by controlling toggling parameters [15, 16].

An emerging question is how an anisotropic shape of particles affects the aggregation kinetics and the microstructural and mechanical properties of MR fluids. The shape anisotropies of magnetic particles give rise to inhomogeneous dipolar interactions and the anisotropic particles are expected to form unique structures [17, 18]. For instance, it has been computationally [19–21] and experimentally [22–24] shown that the structures of ellipsoidal shaped particles or high aspect ratio rods depend strongly on their aspect ratios.

This study employs magnetic ellipsoid-shaped colloids and follows the procedure of earlier microgravity experiments using spherical colloids to investigate the effect of particle shape on the growth of microstructures in MR fluids without particle sedimentation. The external toggled magnetic field is applied to ellipsoid suspension and the effect of toggling process on the growth mechanism of microstructures is observed. The aspect ratio of the magnetic ellipsoids are varied to investigate the effect of particle shape on the assembly kinetics. The ellipsoids have a remnant magnetic moment and allow us to simultaneously study the effect of a permanent dipole attraction between particles.

We find that the magnetic field strength affects the attraction potential, and therefore, the assembly kinetics. However, a combination of contributions from the particle shape and the attraction potential (specifically, the presence of an interaction due to magnetic remanence) results in structural pinning for large aspect ratio ellipsoids, causing less dependence of the field strength and toggling frequency, whereas the particle aggregation kinetics for small aspect ratio ellipsoids depend more strongly on the *external* magnetic field conditions. These results can be rationalized by the number of contacts long versus short ellipsoids are expected to make. Before discussing these results, we first present the experimental materials and methods in the next section.

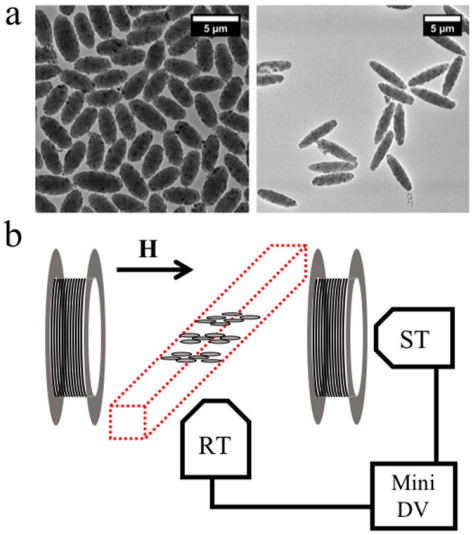

Figure 1. (a) Transmission electron microscope images of magnetic ellipsoids used for experiments with aspect ratio $\alpha = 2$ (left) and $\alpha = 4$ (right). (b) Microgravity glovebox in the International Space Station (ISS) is schematically described. Sample cells are placed at the center (red dotted box) of Helmholtz coils. The microstructure is observed by two ccd cameras, RT and ST, that take images parallel and perpendicular to the applied magnetic field direction, respectively.

2. Experimental

Magnetic ellipsoid particles are fabricated by the method of Ho *et al* [25]. We start with spherical magnetic latex particles (diameter $d = 2.5 \pm 0.27$ μm, Spherotech, Lake Forest, IL), which are polystyrene particles coated with magnetite nanoparticles. The latex particles are dispersed in a polymer solution (polyvinyl alcohol, PVA) and cast into thin films. The films are stretched uniaxially after heating the film above the glass transition temperature of the polystyrene particles, $T_g \approx 95$ °C, in a hot silicone oil bath. After stretching, ellipsoidal particles are recovered from the PVA matrix by dissolving PVA in a 7:3 water–isopropanol solution for 12 h. The solution is centrifuged and the particles are resuspended in the same water–isopropanol solution for 12 h. Next, the solution is heated to 50 °C–60 °C for 1 h. These centrifugation and resuspension steps are repeated three times in water–isopropanol mixture and five times in water. Figure 1(a) shows transmission electron microscope (FEI Talos F200C operating at 200 kV) images of two ellipsoids used in this paper with aspect ratio $\alpha = 2$ and $\alpha = 4$. The lengths in longer (L) and shorter (d) axis of ellipsoids are $d_{\alpha=2} = 1.99 \pm 0.05$ μm, $L_{\alpha=2} = 4.30 \pm 0.12$ μm, $d_{\alpha=4} = 1.66 \pm 0.05$ μm, and $L_{\alpha=4} = 6.57 \pm 0.16$ μm.

Each sample is held in a hermetically sealed glass capillary (inner diameter: 0.70 mm; wall thickness: 0.14 mm; length: approximately 50 mm). Before loading the particle suspension,

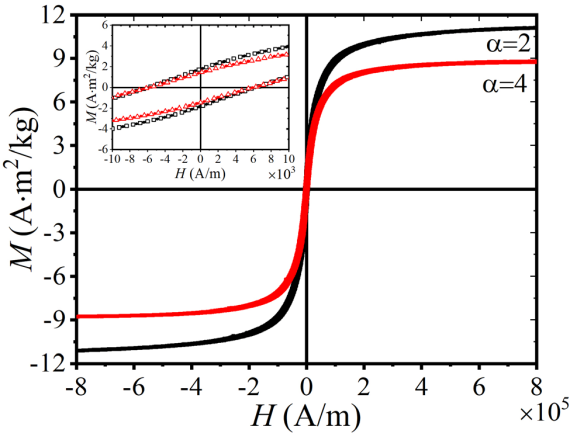

Figure 2. Magnetic properties of ellipsoids and induced dipole–dipole attractive potential. Magnetic moments, M, of ellipsoids measured with vibrating sample magnetometer (VSM) are plotted versus magnetic field, H. Black and red graphs indicate magnetic hysteresis loops for ellipsoids with aspect ratio, $\alpha = 2$ and 4, respectively.

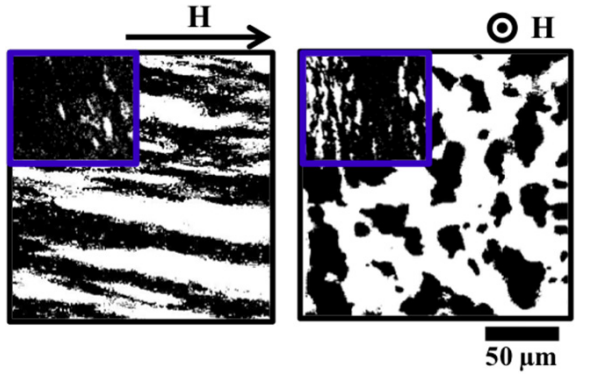

Figure 3. Images of magnetic ellipsoids (0.5% by volume) with aspect ratio $\alpha = 4$ are taken by RT (left) and ST (right) cameras 5 min after turning on external toggled magnetic field with field strength $H = 500$ A m^{-1} and pulse frequency $\omega = 2$ Hz. Insets show samples under no magnetic fields. The images are processed to increase the contrast between particle-rich (black) and particle-poor (white) region. Arrows indicate the direction of the applied magnetic field. Scale bar: 50 μm.

one end of the capillary tube is sealed with an electric welder. The capillary tube is filled with suspension of the synthesized ellipsoids (24.5 μl). The other end is then sealed with acetylene/oxygen torch. Complete sealing is examined by connecting the capillary to a vacuum and checking the pressure drop and flow in the capillary tube.

Figure 1(b) illustrates experimental equipments used in the ISS for microgravity self-assembly experiments. The magnetic ellipsoid suspension is placed at the center of Helmholtz coils to apply toggled magnetic field. The magnetic ellipsoids suspended in water (0.5% by volume) are subjected to toggled magnetic field and microgravity experimental condition on the International Space Station (ISS) allows us to observe microstructure formation driven solely by external field without catastrophic sedimentation of colloidal particles.

For quantitative analysis of magnetic field-driven interaction potentials between magnetic ellipsoids, magnetic properties of particles are measured by vibrating sample magnetometer (VSM). Figure 2 shows magnetization curves for two ellipsoidal particle with different aspect ratios, $\alpha = 2$ (black) and $\alpha = 4$ (red). According to the VSM result, it is noted that aspect ratios affect saturation magnetization as marked by the plateau position of each ellipsoid. Enlarged VSM results shown in the inset reveal that both ellipsoids show remnant magnetization at zero magnetic field. Remnant magnetic moments (M_r) for ellipsoids with $\alpha = 2$ and $\alpha = 4$ are $M_r = 1.8$ A $\cdot$ m^2 kg^{-1} and 1.4 A $\cdot$ m^2 kg^{-1}, respectively.

3. Results and discussion

In all of the experiments, the MR suspensions of ellipsoidal particles exhibit a transition from a system-spanning state in the absence of an external magnetic field to collapsed structures in a magnetic field ($H = 500$ A m^{-1}), as shown by snapshots of the experiments in figure 3. In figure 3, images showing parallel (RT view, left) and perpendicular (ST view, right) view to the applied magnetic field represent microstructure formation 5 min after turning on the toggled magnetic field. The initial state of the magnetic ellipsoid suspension with no magnetic field in insets shows that the magnetic ellipsoids create few particle aggregated regions and the aggregates and stable particles are homogeneously distributed over the sample. This aggregation can be attributed to remnant magnetization of the magnetic ellipsoids. When the external magnetic field is applied, the suspension begins aggregating and forming microstructures. The aggregates are column-like in shape from the RT and have a roughly circular cross-section when viewed by the ST camera.

The initial structure and its evolution in the externally applied field can be understood in terms of the magnetic particle interactions. Since the magnetic fields used in the experiments ($H = 500$–1500 A m^{-1}) are in a range for which the magnetic moment is linearly proportional to the applied magnetic field, χ, the dipole–dipole interaction potential between two ellipsoids can be estimated by the magnetic susceptibility χ and the approximate expression of the point dipole model

$$U_{\alpha\beta} = \frac{1}{4\pi\mu_0 r_{\alpha\beta}^3}(\mathbf{I} - 3\hat{\mathbf{r}}_{\alpha\beta}\hat{\mathbf{r}}_{\alpha\beta}) : \mathbf{m}_\alpha\mathbf{m}_\beta \qquad (1)$$

where μ_0 is the vacuum permeability, $r_{\alpha\beta}$ is the center-to-center distance between two particles, $\hat{\mathbf{r}}$ is the unit vector between two particle centers. $\mathbf{m}_\alpha$ is the magnetic moment of spherical particle α, which is defined as $\mathbf{m}_\alpha = \frac{4}{3}\pi a^3\mu_0\chi\mathbf{H}$ for a magnetic particle of the radius a. Given the remnant magnetic moment M_r and particle shape, the magnetic moment is expressed as $\mathbf{m}_\alpha = V_p\mu_0(\chi\mathbf{H} + \mathbf{M}_r) = \frac{4}{3}\pi a^2 L\mu_0(\chi\mathbf{H} + \mathbf{M}_r)$, where L and a refer to the length half of the ellipsoid length and diameter, respectively. When two of the same magnetic particles α are contacted at their surface, the dipole–dipole interaction potential can be calculated using

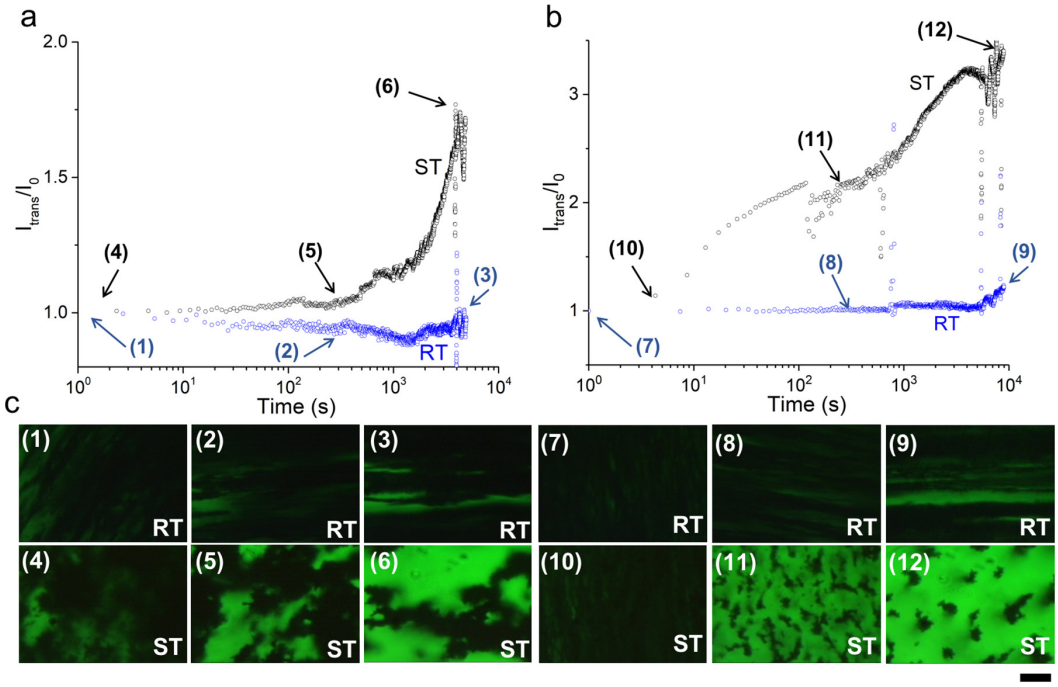

Figure 4. Transmitted light intensity depending on the field-applied time. Transmitted light intensities (I_{trans}) through the samples of (a) ellipsoids with aspect ratio, $\alpha = 2$ and (b) $\alpha = 4$ from ST (black open rectangles) and RT (blue open circles) are estimated as a function of magnetic field-applied ($H = 500$ A m^{-1} and $\omega = 2$ Hz) time. Intensities are normalized by the initial light intensity (I_0). (c) Images show aggregated microstructures corresponding to each state indicated by arrows with numbers in (a) and (b). Scale bar: 50 μm.

$$\lambda = \frac{U}{k_B T} = \frac{(1 - 3\cos^2\theta) m_\alpha^2}{4\pi\mu_0 r^3 k_B T}, \tag{2}$$

where the center-to-center distance r is

$$r = 2\sqrt{\frac{a^2 L^2}{a^2\cos^2\theta + L^2\sin^2\theta}}.$$

The dimensionless dipole strength λ is normalized by the Boltzmann thermal energy ($k_B T$), a product of Boltzmann constant k_B and temperature T. The dipole strength characterizes the assembly behavior. When magnetic interactions are strong and the dipole strength is $\lambda \gg 1$, the magnetic particles form microstructures due to the dominant dipole–dipole interaction. When $\lambda \ll 1$, they are normally dispersed by Brownian motion. However, the remnant magnetic potential (see figure S1, available in the online supplementary material (stacks.iop.org/JPhysD/52/184002/mmedia)) induces an interaction on the order of $34k_B T$ for the $\alpha = 2$ ellipsoids and $13k_B T$ for the $\alpha = 4$ ellipsoids. This means that the magnetic ellipsoids tend to aggregate and form a percolated microstructure in the absence of the toggled magnetic field, which agrees with the observation presented in the ST view of figure 3 (inset).

Further details of the structure formation are shown in figure 4, in which we plot both the total intensity of transmitted light through the samples and the RT and ST views of the suspension microstructures for ellipsoids with $\alpha = 2$ and 4 in figures 4(a) and (b), respectively. As discussed previously, the suspension structures of both ellipsoid aspect ratios coarsen, forming column-like bodies. Only a small amount

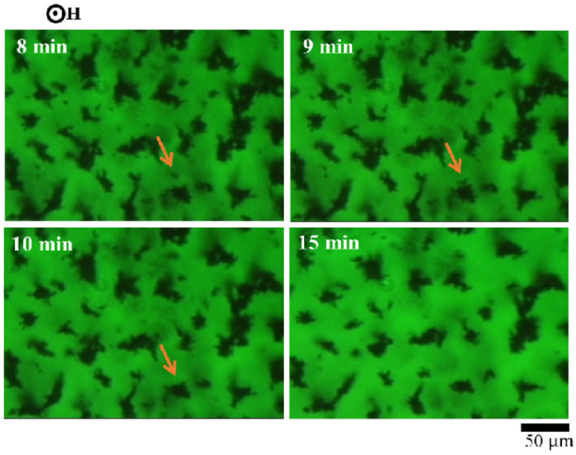

Figure 5. Coalescence of magnetic ellipsoid columns. Magnetic ellipsoids (0.5% by volume) with aspect ratio $\alpha = 4$ are at $H = 500$ A m^{-1} and $\omega = 2$ Hz. Orange arrows indicate merging two coalesced columns. The direction of applied magnetic field is normal to image plane. Scale bar: 50 μm.

of light penetrates in the RT view, a notable difference to previous experiments with paramagnetic spheres, in which the column width could be monitored [6]. This indicates that the structure is unable to fully condense, likely due to the dipolar interactions induced by the remanent polarization of the ellipsoids. Nonetheless, intriguing differences are observed for the two aspect ratios. Due to stronger magnetic remanence of ellipsoids with $\alpha = 2$ as shown in figure S1, particles are

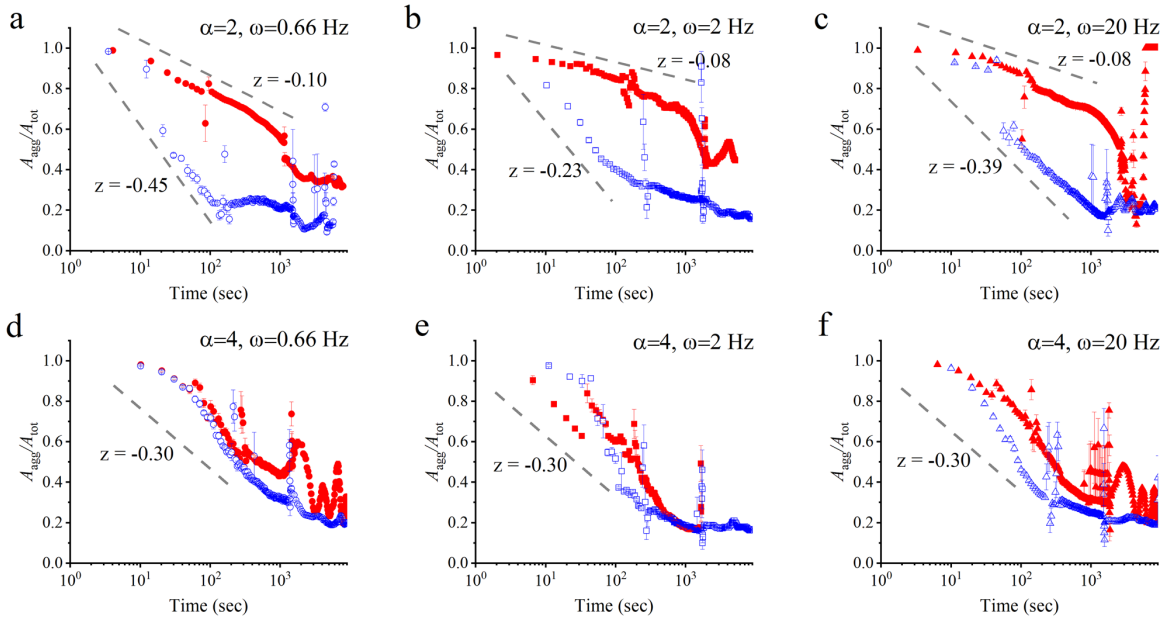

Figure 6. Particle distribution under the external magnetic field. The magnetic ellipsoids (0.5% by volume) aggregated area, A_{agg}, is plotted versus time, t. Area is normalized by the total area of the screen, A_{tot}. A_{agg}/A_{tot} values for ellipsoids with aspect ratio (a)–(c) $\alpha = 2$ and (d)–(f) $\alpha = 4$ are displayed at different magnetic field strengths, $H = 500$ A m^{-1} (red close rectangles) and 1500 A m^{-1} (blue open rectangles). Toggling frequency (ω) is set to (a), (d) 0.66 Hz, (b), (e) 2 Hz, or (c), (f) 20 Hz. Gray dashed lines illustrate the power-law behavior in the initial stage of microstructure growth.

initially more aggregated than higher aspect ratio ellipsoids according to initial aggregated microstructure formed under no magnetic field in figure 4(c). When viewed along the field direction (ST view), the smaller aspect ratio ellipsoids form large aggregates, while the longer ellipsoids form many more smaller and dispersed columns. The total transmitted intensity captures these differences too. The intensity for $\alpha = 4$ (figure 4(b)) increases more rapidly than the $\alpha = 2$ sample after the application of the field, consistent with more disperse microstructures. In addition to lateral coalescence of the columns in this case, the intensity of transmitted light between columns increases, indicating that the columns are growing in length, as well. One mechanism for coarsening appears to be lateral coalescence between the columns, which is observed periodically within the field of view. An example is illustrated in figure 5. The time between images is shorter in figure 5 (structures between 8 min and 15 min), which was only intended to illustrate a coalescence event. Over longer times, the number of aggregates in the field of view decreases, consistent with figure 4.

Next, we analyze the area occupied by aggregates over the total image area, A_{agg}/A_{tot} from ST view images as a function of time the field is applied. (Figure S2 presents the corresponding RT data, which exhibit little change, consistent with the images in figure 4(a).) Again, due to the magnetic interaction between particles and the lateral interaction between columnar aggregates, the microstructure coarsens. The normalized area of the aggregates decreases (figure 6). For ellipsoids with short aspect ratio ($\alpha = 2$), the change in aggregate area depends strongly on field strength; coarsening occurs more rapidly at $H = 1500$ A m^{-1} than 500 A m^{-1}.

For small aspect ratio particles, the initial growth kinetics exhibits a power-law like trend, so the exponents z are estimated over an initial region of growth (reported in table S1). The fastest kinetics, which occur at the higher field strength, exhibit power laws on the order of ~0.23–0.45, which is close to 0.3 for diffusion-mediated coarsening [26], but with intermittent coalescence events that were illustrated earlier. Such a thermal process is similar to the coarsening kinetics that are observed in studies of MR suspensions of spherical particles [6]. At the lower field strength, slower growth kinetics dominate, where $z \sim 0.1$. This is attributed to strong magnetic remanence which in turn, requires stronger magnetic strength to overcome the potential causing particle aggregation.

For longer ellipsoids ($\alpha = 4$), there is little difference in the coarsening process at different field strengths. The effect of toggle frequency also depends on the particle aspect ratio. Short ellipsoids exhibit a modest dependence on the toggle frequency. At $\omega = 0.66$ Hz, the suspensions coarsen more quickly, while coarsening slows as the frequency increases to 2 and 20 Hz. This dependence is more clearly seen when the results are plotted together in figure 7(a). Again, in contrast, longer ellipsoids exhibit little dependence on toggle frequency (see figure 7(b)).

Another feature of the aggregate area plots are periodic oscillations at long times (figure 6). These oscillations are attributed to the precession of the aggregates in the Earth's magnetic field. The aggregates tilt depending on the location of the ISS, and their size in the ST view grows or shrinks. The period of the oscillation is approximately 2700 s, equivalent to one half of the ISS orbital period [27]. The emergence of this oscillation is a strong indicator that the length of the aggregates

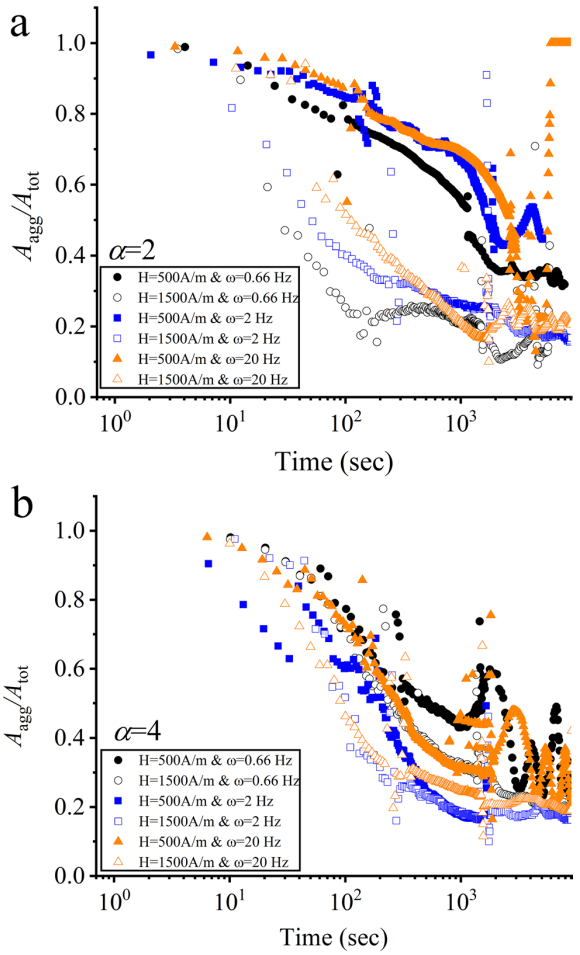

Figure 7. ST view of microstructures under pulsed magnetic fields. From the ST camera, particle distributed areas of the ellipsoids with aspect ratio (a) $\alpha = 2$ and (b) $\alpha = 4$ shown in figure 6 are overlapped for the comparison and presented as the aggregate size (A_{agg}) normalized by the total area of the screen (A_{tot}) versus pulse field applied time. Black circles, blue rectangles, and orange triangles indicate pulse field frequency, $\omega = 0.66$ Hz, 2 Hz, and 20 Hz, respectively. Open and closed symbols refer to the field strength $H = 500$ A m^{-1} and $H = 1500$ A m^{-1}, respectively.

increases with time, since this would lead to a larger magnetic moment that ultimately follows the direction of the weaker field of the Earth, much like a compass needle. The noise at the end of each measurement is the result of a translation of the sample to observe the overall structures throughout the suspension. These confirm that there are no large variations or differences throughout the observable volume of the sample.

The results of these studies are different than the toggled-field assembly of paramagnetic spheres under microgravity conditions, in which strong phase separation occurred with time to form larger and more defined columnar and droplet-like structures [6]. Instead, the coarsening of the ellipsoid samples behaves more like the structural evolution of paramagnetic suspensions in dc magnetic fields [9, 28–30]. This effect is likely due to the strong dipolar interactions of the particles' remanent magnetic interaction, which persist even as the field toggles off. The attractions limit their diffusive rearrangement that is the hallmark of the annealing process for paramagnetic suspensions. However, there are interesting and distinct differences in the behavior of ellipsoids with different aspect ratios. Toggling the field has an effect on shorter aspect ratio ellipsoids, but not on longer ones, and the aggregated structures for the shorter ellipsoids are larger and less dispersed as individual columns. We attribute this difference to the higher contact number of the longer ellipsoidal particles. In their studies of self-assembling attractive Janus ellipsoids, Shah and coworkers found that only high aspect ratio ellipsoids ($\alpha > 3.5$) form structured fibers [24]. This aspect ratio regime in which ellipsoids form high contact number phase includes the high aspect ratio ellipsoid ($\alpha = 4$). Thus, we expect that high aspect ratio ellipsoids first assemble into a fiber structure which is pinned by their remanent dipolar interactions. Consequently, the pinning results in less dependence of the aggregation rate on magnetic strength and toggling frequency, through a lateral fiber–fiber aggregation mechanism.

4. Conclusions

Colloidal interactions induced by magnetic and electric fields are important for the formation of microstructure and response of magneto- and electrorheological fluids. Fields, when toggled, can also be harnessed for directed particle self-assembly. In this work, we studied driven suspensions of anisotropic magnetic nanoparticles free from gravitational sedimentation. The attractive interactions between the ellipsoids due to their magnetic remanence lead to microstructures which are not fully dispersed. Toggling the field does not lead to phase separation as it does for paramagnetic suspensions. Nonetheless, the toggled field does cause the suspension to coarsen. The kinetics of coarsening and effects of field strength and frequency depend on the aspect ratio of the particles. Although they are prevented from fully redispersing when the field is off, shorter aspect ratio ellipsoids may rearrange more. Long ellipsoids coarsen in a manner similar to paramagnetic colloids in dc fields, suggesting that their microstuctures are 'pinned' more by a higher number of contacts between particles. These results provide tantalizing clues to how the interplay between particle shape and external fields can be used to drive structural evolution in magnetic suspensions.

Acknowledgments

We thank P Pfleiderer and J Vermant for fabricating the ellipsoid particles. Funding from NASA (NNX16AD21G and NNX10AE44G) and the NSF (CBET-1637991) are gratefully acknowledged.

ORCID iDs

Hojin Kim https://orcid.org/0000-0001-5922-2490
Eric M Furst https://orcid.org/0000-0002-8849-4484

References

[1] Winslow W M 1949 *J. Appl. Phys.* **20** 1137–40
[2] Larson R G 1999 *The Structrue and Rheology of Complex Fluids* (Oxford: Oxford University Press)
[3] Gast A P and Zukoski C F 1989 *Adv. Colloid Interface Sci.* **30** 153–202
[4] Carlson J D and Jolly M R 2000 *Mechatronics* **10** 555–69
[5] Spencer B F, Dyke S J, Sain M K and Carlson J D 1997 *J. Eng. Mech.* **123** 230–8
[6] Swan J W *et al* 2012 *Proc. Natl Acad. Sci.* **109** 16023–8
[7] Swan J W, Bauer J L, Liu Y and Furst E M 2014 *Soft Matter* **10** 1102–9
[8] Halsey T C and Toor W 1990 *J. Stat. Phys.* **61** 1257–81
[9] Furst E M and Gast A P 1998 *Phys. Rev.* E **58** 3372–6
[10] Hynninen A P and Dijkstra M 2005 *Phys. Rev. Lett.* **94** 8–11
[11] Promislow J H E and Gast A P 1996 *Langmuir* **12** 4095–102
[12] Promislow J H E and Gast A P 1997 *Phys. Rev.* E **56** 642–51
[13] Bauer J L, Liu Y, Kurian M J, Swan J W and Furst E M 2015 *J. Chem. Phys.* **143** 074901
[14] Bauer J L, Kurian M J, Stauffer J and Furst E M 2016 *Langmuir* **32** 6618–23
[15] Sherman Z M and Swan J W 2016 *ACS Nano* **10** 5260–71
[16] Sherman Z M and Swan J W 2019 *ACS Nano* **13** 764–71
[17] Glotzer S C and Solomon M J 2007 *Nat. Mater.* **6** 557–62
[18] Grzelczak M, Vermant J, Furst E M and Liz-Marzán L M 2010 *ACS Nano* **4** 3591–605
[19] Bautista-Carbajal G, Moncho-Jordá A and Odriozola G 2013 *J. Chem. Phys.* **138** 064501
[20] Frenkel D and Mulder B 1985 *Mol. Phys.* **55** 1171–92
[21] Odriozola G 2012 *J. Chem. Phys.* **136** 134505
[22] Solomon M J and Spicer P T 2010 *Soft Matter* **6** 1391–400
[23] Wilkins G M H, Spicer P T and Solomon M J 2009 *Langmuir* **25** 8951–9
[24] Shah A A, Schultz B, Zhang W, Glotzer S C and Solomon M J 2015 *Nat. Mater.* **14** 117–24
[25] Ho C C, Keller A, Odell J A and Ottewill R H 1993 *Colloid Polym. Sci.* **271** 469–79
[26] Siggia E D 1979 *Phys. Rev.* A **20** 595–605
[27] National Aeronautics and Space Administration 2015 *Reference Guide to the International Space Station* (US Government Publishing Office)
[28] Promislow J H E, Gast A P and Fermigier M 1995 *J. Chem. Phys.* **102** 5492–8
[29] Fermigier M and Gast P A 1992 *J. Magn. Magn. Mater.* **122** 46–50
[30] Wirtz D and Fermigier M 1994 *Phys. Rev. Lett.* **72** 2294–7